

Schauer and P. Williams, *Int. J. Mass. Spectrom. Ion. Proc.* 103, 21 (1990)] that by collection of only ions ejected from the sample with energies >300 eV, most molecular species, including hydrides, can be effectively eliminated from the secondary ion spectrum to the part per million level. We counted ions with >350 ± 20 eV, which gave ≈4 E5 counts per second for ¹⁶O on the garnets in this study. Total analysis time was 45 min. Typically, we used 100 cycles, which resulted in craters 5 to 7 μm deep. The error expected from counting statistics ranged from 1 to 1.2 per mil (1 SD). Actual errors clustered between 1 and 1.6 per mil, and two analyses showed larger errors. We converted raw ratios to absolute values by comparing values with those of several natural mineral standards and by assuming a linear relation between instrumental oxygen isotope fractionation and molecular weight of the sample. Plain horizontal lines give average core and rim compositions, and the dashed horizontal lines on the figure represent the oxygen isotope composition obtained for bulk separates of cores and rims analyzed by conventional techniques. The shaded region denotes the relatively grossular-rich core.

20. Fluorine microanalyses were done with a 0.5-nA ¹⁶O⁻ primary beam focused onto a spot 20 μm in diameter. Negative secondary ions with 50 ± 20 eV excess kinetic energy were detected. The ¹⁹F⁻ count rate was normalized to the count rate for ¹⁸O, and this ratio was calibrated against Durango apatite. Previous studies in this lab show small matrix effects (≈15%) for F over a range of phases, presumably because F is nearly com-

pletely ionized during sputtering [P. Williams, in *Practical Surface Analysis*, D. Briggs and M. P. Seah, Eds. (Wiley, New York, 1992), pp. 177–228]. Error of measurements is within the size of the circles.

21. Rare earth element analyses by ion microprobe were done with the duoplasmatron source to generate a ~1.5-nA ¹⁶O primary ion beam at 12.5 kV focused onto a spot 20 μm in diameter. Positive secondary ions of ⁴²Ca, ¹³⁹La, ¹⁴⁰Ce, ¹⁴³Nd, ¹⁴⁷Sm, and ¹⁶⁶Er with 75 ± 20 eV excess energy were detected. Erbium contents were corrected for oxides of Nd and Sm, and concentrations were determined according to the methods described by E. Zinner and G. Crozaz [*Int. J. Mass. Spectrom. Ion. Proc.* 69, 17 (1986)]. Errors (1 SD) of individual measurements were determined by counting statistics. Data tables are available from the authors on request.
22. A. J. Kemp, A. J. Lewis, M. R. Palmer, in preparation.
23. Neodymium isotope data were obtained at the Mineralogical-Geological Museum in Oslo. Isotopic ratios were measured on a VG 354 5-collector fully automated mass spectrometer. Analytical methods follow the procedures described by E. W. Mearns [*Lithos* 19, 269 (1986)].
24. B. Jamtveit, unpublished results.
25. We thank K. V. Ragnarsdottir for help with the ICP analyses and J. Blundy, K. V. Ragnarsdottir, and R. Wogelius for comments on the manuscript. Supported by the Norwegian Research Council (440.92/023 and 440.93/011).

20 August 1993; accepted 2 December 1993

Glacial-Interglacial Changes in Moisture Sources for Greenland: Influences on the Ice Core Record of Climate

C. D. Charles, D. Rind, J. Jouzel, R. D. Koster, R. G. Fairbanks

Large, abrupt shifts in the ¹⁸O/¹⁶O ratio found in Greenland ice must reflect real features of the climate system variability. These isotopic shifts can be viewed as a result of air temperature fluctuations, but determination of the cause of the changes—the most crucial issue for future climate concerns—requires a detailed understanding of the controls on isotopes in precipitation. Results from general circulation model experiments suggest that the sources of Greenland precipitation varied with different climate states, allowing dynamic atmospheric mechanisms for influencing the ice core isotope shifts.

A network of ice cores now spans much of the Greenland ice sheet. The δ¹⁸O records from the ice cores reveal a pattern of pronounced, abrupt shifts prior to the Holocene period (1). The fact that many shifts can be traced among different cores makes

it clear that these oscillations are not merely artifacts of local ice sheet dynamics. Yet, their climatic implications have not been fully resolved. Comparison with the δ¹⁸O-temperature correlation established from modern precipitation (2) implies that the δ¹⁸O shifts, in some cases, reflect temperature fluctuations of 7° to 10°C occurring over the course of less than 20 years (3). Obvious questions arise from this type of inference: (i) What aspects of the climate system are capable of creating such large temperature fluctuations over such a broad area and so rapidly? (ii) Can such temperature shifts be triggered in the modern climate through anthropogenic influences?

These oscillations in δ¹⁸O are usually considered to be driven primarily by the North Atlantic because experiments with a

coupled ocean-atmosphere model suggest that the North Atlantic thermohaline circulation, which delivers heat to the high latitudes, could alternate between two stable modes of operation (on or off), and aspects of North Atlantic deep-sea sediment records exhibit this type of behavior (4). However, several observations also suggest the involvement of other climatic processes. In a series of model experiments that effectively tested the sensitivity of climate to reduced North Atlantic heat transport, this mechanism could explain less than one-third the magnitude of air temperature change over Greenland inferred from the ice core isotopic shifts (5). Recent estimation of the rapidity of the changes in the ice cores (6) suggests that the variations occur more rapidly than do variations in European climate records that are undeniably the product of North Atlantic surface ocean changes (7). New dating of the ice core record at Summit suggests that two of the most prominent δ¹⁸O shifts occur precisely during catastrophic melting of the ice sheets, at about 14,000 and 11,000 years ago (8). Thus, it seems unlikely that the North Atlantic acted alone to shape the dramatic ice core records.

To comprehend the full climatic significance of the δ¹⁸O events, we must establish the driving forces for isotopic variability in precipitation. Although the fractionation of H₂¹⁸O between water vapor and condensate is temperature dependent, the amount of H₂¹⁸O in precipitation at any given location is more directly determined by the amount of original vapor remaining in the air mass (9). Because colder air holds less water vapor, this distillation process also depends on temperature, but the correlation between δ¹⁸O and temperature varies according to the location of the original moisture sources (whether it is remote or proximal), the trajectories of the moisture (whether it is advected along a cold or warm path), and the mixing between sources with different degrees of distillation. Thus, local δ¹⁸O variability may result from a combination of direct air-temperature effects and complicated air mass mixing effects. These influences must be separated for accurate paleoclimatic reconstruction. More importantly, regardless of how the modern δ¹⁸O-temperature calibrations apply to the rapid shifts observed in the ice cores (10), the causes of the shifts cannot be deduced from empirical extrapolations. One must also understand where and how the characteristics of moisture sources changed under different climate conditions.

One approach is to use a general circulation model (GCM) that is capable of considering explicitly the complex variety of processes that act on the isotopes. Previous GCM studies indicated that although

C. D. Charles, Scripps Institution of Oceanography, University of California at San Diego, La Jolla, CA 92093.

D. Rind, Goddard Institute for Space Studies, New York, NY 10028.

J. Jouzel, Laboratoire de Modelisation du Climat et de l'Environnement, CEA/DSM CE Saclay, 91191 Gif Sur Yvette, France, and Laboratoire de Glaciologie et Geophysique de l'Environnement, CNRS BP96, 38402, Saint Martin d'Heres Cedex, France.

R. D. Koster, Hydrological Sciences Branch, National Aeronautics and Space Administration/Goddard Space Flight Center, Greenbelt, MD 20904.

R. G. Fairbanks, Lamont-Doherty Earth Observatory, Palisades, NY 10964, and Department of Geological Sciences, Columbia University, New York, NY 10025.

changes in precipitation site temperature explained much of the glacial-interglacial isotopic variability in polar regions, the isotopes were also sensitive to persistent changes in atmospheric circulation (11). In this report, we present determinations of moisture sources and their isotopic influences for Greenland precipitation made with the Goddard Institute for Space Studies (GISS) GCM, comparing the results from modern (control) and last glacial maximum (LGM) experiments.

We used a version of the GISS model with nine vertical layers, 4° by 5° resolution, and prescribed sea surface temperatures (SSTs) (12). Boundary conditions (ice sheet extent, sea ice extent, and SSTs) for the LGM experiment were interpolated from CLIMAP (13) reconstructions. The isotope tracer component of the GISS GCM applies the appropriate fractionation equations at every change of phase for water in the model and keeps track of the total mass of various isotopes in all potential reservoirs (for example, vapor, precipitation, ground water, and ice) (14). Moisture sources for any given region can also be determined because water molecules (including the isotope species) evaporating from specified grid boxes can be treated as a tracer and followed until precipitation (15). This model capability provides an important advantage because it is rarely possible to determine sources of local precipitation in the real world.

Annual average precipitation over Greenland in the modern experiment was derived from a wide variety of source regions (Fig. 1). The contributions to high-elevation precipitation were fairly evenly divided between a North Atlantic source (20 to 25%), a Norwegian Sea–Greenland Sea source (15 to 20%), a North American source (15 to 20%), and a North Pacific source (15 to 20%). A more minor contribution is made by tropical Atlantic sources (5 to 10%). Other source regions (Eurasia, tropical Pacific, and Greenland itself) also supply small but detectable amounts of moisture. Labrador Sea and Arctic Ocean sources appear to be important only for coastal precipitation.

The pattern of sources varied seasonally in the modern experiment (Table 1). For example, the North American contribution to Greenland precipitation comes almost exclusively in summer, when high rates of continental evapotranspiration fuel the cyclones that track eastward across the ice sheet. Cooler winter SSTs and seasonal sea ice cover reduce the contribution of the Norwegian–Greenland Sea source from November through April. This change effectively increased the relative importance of the North Atlantic and North Pacific sources, which appear more steady. Over-

all, the seasonally variable combination of distal and proximal, oceanic and continental sources for Greenland precipitation in

the GISS GCM provides an entirely different picture than that of simple models, in which it is assumed explicitly that the

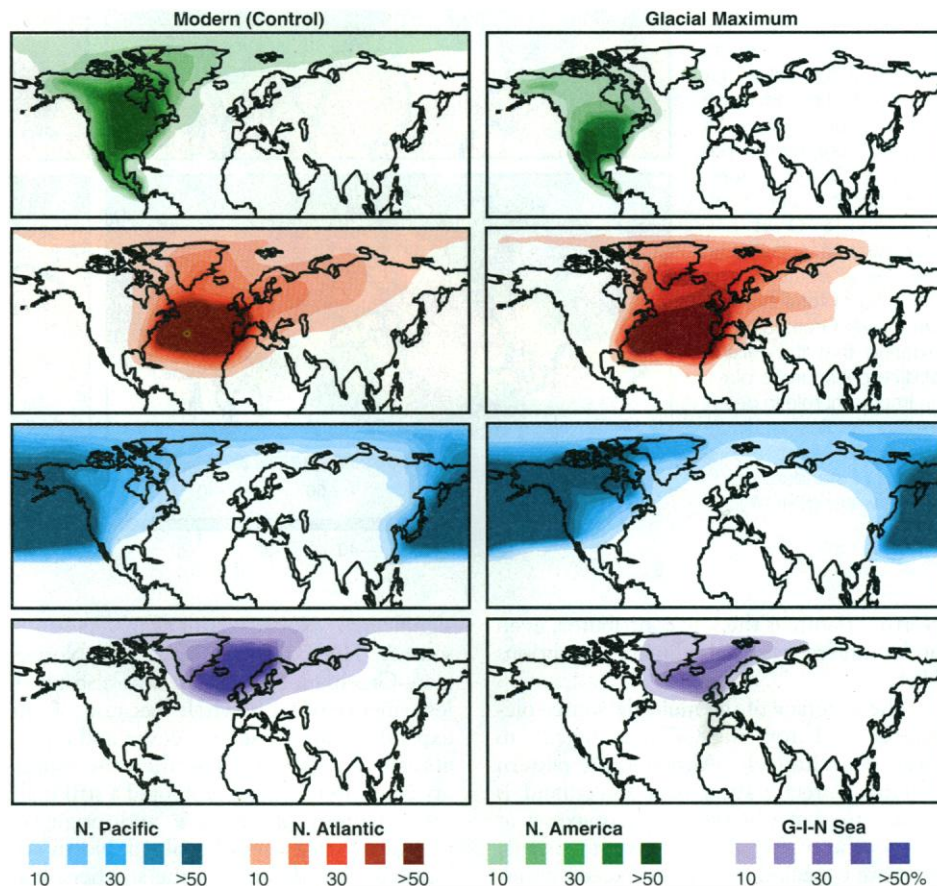


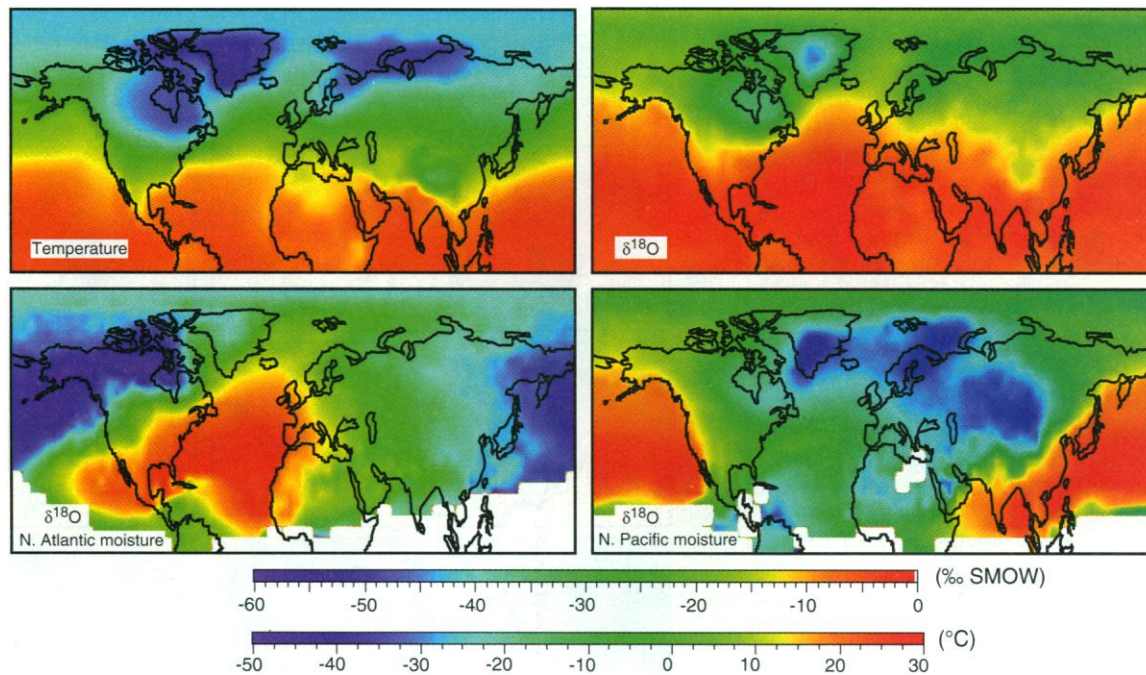
Fig. 1. Percent contributions of various moisture sources to local mean annual precipitation, calculated at every grid box as mass of source tracer precipitated per mass of total precipitation times 100. Results are averaged over 2-year simulations. This approach is analogous to mapping the intensity of a dye that tags moisture evaporating from a specified set of grid boxes. For example, heavy red shading over a region indicates that a high proportion of total precipitation in that region (not global precipitation) was originally evaporated from the North Atlantic. Results from the modern simulation (left panels) show that Greenland precipitation is derived from a complex variety of sources and is not dominated by any one source. The glacial simulation (right panels) results show a zonal distribution: north Greenland precipitation is dominated by North Pacific moisture and south Greenland is dominated by North Atlantic moisture.

Table 1. Contribution of different source areas to Greenland Summit precipitation in a 2-year simulation. Results from modern experiment are given, and the results from the ice age experiment are in parentheses.

Source area	Contribution* (%)				
	Winter	Spring	Summer	Fall	Average
	<i>Modern (Glacial)</i>				
Greenland	1 (0)	3 (2)	11 (9)	4 (0)	6 (2)
Norwegian-Greenland Sea	21 (4)	19 (8)	7 (14)	22 (19)	18 (11)
Labrador Sea	1 (1)	1 (1)	1 (1)	2 (1)	2 (1)
North America (Canada)	0 (0)	3 (0)	22 (0)	8 (0)	7 (0)
North America (other)	4 (4)	10 (8)	13 (8)	6 (4)	7 (6)
North Atlantic (30° to 50°N)	31 (38)	18 (40)	12 (35)	20 (38)	26 (38)
Tropical Atlantic (30°N to 30°S)	11 (15)	10 (10)	8 (5)	5 (7)	6 (11)
North Pacific (>30°N)	16 (22)	15 (13)	8 (8)	22 (20)	13 (15)
Eurasia	2 (3)	5 (10)	12 (12)	8 (6)	6 (7)
Arctic Ocean	2 (2)	1 (1)	1 (2)	1 (1)	1 (1)
Other	11 (11)	14 (7)	5 (6)	4 (4)	8 (8)

*Average of four grid boxes that have elevations in the modern experiment of close to 3000 m.

Fig. 2. Predicted mean annual fields for surface temperature (lower color scale) and $\delta^{18}\text{O}$ (upper color scale) from the glacial experiment. The lower panels show the mean annual $\delta^{18}\text{O}$ value for North Atlantic and North Pacific sources alone. A general congruence between $\delta^{18}\text{O}$ and temperature can be seen; however, the $\delta^{18}\text{O}$ of neither Atlantic nor Pacific sources is equivalent to the $\delta^{18}\text{O}$ of total precipitation over Greenland, indicating that the mixing of different sources plays an important role in determining the final balance. The $\delta^{18}\text{O}$ values are in per mil of standard mean ocean water (SMOW).



North Atlantic is the sole contributor, even under different global climate conditions (16).

The accuracy of the multiple-source picture derived from the GCM is difficult to assess quantitatively. Although the pattern of model precipitation over Greenland is similar to that observed, with maxima at the southern and the northwest corners, estimated precipitation rates exceed observations by as much as 100% (1 mm per day), especially in summer (17). This overestimation is common to a number of GCMs and is largely independent of grid resolution or advective scheme (18). Yet, aside from this comparison of absolute rates, there is little evidence with which to evaluate the calculated relative contributions from any particular source. The model simulates nicely the observed distribution of stable isotope ratios in the mid-latitudes, where the relative amount of local (versus distilled) moisture controls a significant component of the variability (19). In any case, even though the exact apportionment may be questioned, we have no reason to believe that the existence of multiple moisture sources for Greenland precipitation is an artifact.

The ice age experiment produced fairly predictable changes in the contribution of moisture source regions (Fig. 1). Annual average precipitation for Greenland was reduced by a factor of 3 to 10 relative to the modern simulation; this reduction fell within the range of estimates for observed changes in glacial-interglacial accumulation rate (20). Part of this change in the model reflects the fact that the imposition of a Laurentide ice sheet eliminated any

significant North American moisture source. The contribution of the Norwegian–Greenland Sea source was also much less important as a whole because of the expanded summer sea ice cover and cooler annual average SSTs. Together, the boundary condition changes promoted a strikingly zonal pattern of air flow and origin of moisture source over Greenland: North Atlantic sources dominated the southern part of the ice sheet, whereas North Pacific sources dominated the northern. The zonality was more sharply delineated because the North American source, representing a recycled mixture of both North Atlantic and North Pacific moisture, was not a factor in the LGM experiment.

If real, this type of moisture source change could wield a significant isotopic effect. For example, in the model, moisture from the North Pacific source arrives at the Greenland coast with a $\delta^{18}\text{O}$ value roughly 15 per mil lower than its North Atlantic counterpart (Fig. 2). The lower $\delta^{18}\text{O}$ results from the fact that North Pacific moisture is advected along a much colder path before reaching Greenland, and thus, the degree of isobaric cooling is much greater than for North Atlantic air parcels. As an extreme example of the potential effect of mixing of these moisture sources, a $\delta^{18}\text{O}$ anomaly of 7 per mil would be generated if no other climate changes (including temperature) besides a shift from pure North Atlantic contribution to an even mixture of North Atlantic and Pacific moisture occurred. The GCM results in Table 1 are not suggestive of such extreme moisture source shifts over central Greenland, and in any case, changes in the influence of different

air masses would probably also bring about some air temperature change. However, alternation between the dominance of Pacific moisture during glacial periods—typical of northern Greenland in the model results—and admixtures of less isotopically distilled sources may explain questions such as why the average amplitude of the $\delta^{18}\text{O}$ shifts in the Camp Century ice core (northwest Greenland) is much larger than that in the Summit (central Greenland) or Dye 3 (southern Greenland) cores (21).

Yet, changes in the origin of moisture sources or air mass mixing would have implications for the ice core records beyond the uncertainty introduced to the $\delta^{18}\text{O}$ -temperature relation. Additional climatic influences on the ice core record must be explored. For example, the distilling and orographic steering capacity of the Laurentide ice sheet (22) could dictate the distribution, intensity, and isotopic composition of North Pacific moisture throughout the Arctic region. Conceivably, through this shadow effect, the abrupt ice core $\delta^{18}\text{O}$ anomalies might be as much a reflection of Laurentide ice sheet dynamics as North Atlantic surface ocean variability. Furthermore, air mass or moisture source changes provide one plausible mechanism for the strong coupling between the abundance of isotopes and particulates in the ice cores (23). Finally, our model results, combined with the observations of Alley *et al.* (6), make it likely that the abrupt $\delta^{18}\text{O}$ anomalies reflect local dynamical responses of the atmosphere, as opposed to hemisphere-wide changes in energy balance.

In conclusion, GCM experiments suggest that, unlike Antarctica or other conti-

mental regions (24), Greenland is influenced by a heterogeneous collection of moisture sources. The ultimate signature of these moisture sources is determined by a variety of climate processes, and therefore, meaningful interpretation of the Greenland ice core record, including the implications for future climate, can only be achieved by appeal to a multidimensional perspective.

REFERENCES AND NOTES

- S. J. Johnsen *et al.*, *Nature* **359**, 311 (1992).
- W. Dansgaard *et al.*, *Tellus* **16**, 436 (1964).
- W. Dansgaard *et al.*, *Nature* **339**, 532 (1989).
- W. S. Broecker *et al.*, *ibid.* **315**, 21 (1985); S. Manabe and R. J. Stouffer, *J. Clim.* **1**, 841 (1988).
- The magnitude of the air temperature response over Greenland to the imposition of glacial-like North Atlantic SSTs in the GISS GCM was about 2°C [D. Rind *et al.*, *Clim. Dyn.* **1**, 3 (1986)]. Central and northwest Greenland (1) and the Canadian Arctic ice cores [R. M. Koerner *et al.*, *Can. J. Earth Sci.* **24**, 296 (1987)] show some of the most striking isotopic changes, yet seem removed from direct North Atlantic influence in these GCM simulations.
- R. Alley *et al.*, *Nature* **362**, 527 (1992).
- Isotopic records from the German pine tree ring series [B. Becker *et al.*, *ibid.* **353**, 647 (1991)] and the Lake Goszcz (Poland) varved-sediment record [K. Rosanski *et al.*, in *The Last Deglaciation: Absolute and Radiocarbon Chronologies*, E. Bard and W. S. Broecker, Eds. (Springer-Verlag, Berlin, 1992), pp. 69–80] suggest that the Younger Dryas–PreBoreal transition occurred over the course of about 100 years in Europe. This contrasts with the estimate of less than 10 years for the same event in the Summit ice cores (6).
- Dates for the Younger Dryas–PreBoreal transition in the Greenland Ice-Core Project (GRIP) and Greenland Ice Sheet Project-2 (GISP2) ice cores at Summit average 11,550 years ago (1, 7). This age, determined by annual layer counting, is identical (within analytical uncertainties) to the age of the second pulse of ice sheet melting apparent in the Barbados sea level [11,400 years ago by U/Th dating, E. Bard *et al.*, *Nature* **345**, 405 (1990); (25)]. Similar correspondence (though with greater age uncertainty) exists for the “Glacial-Bolling” transition at about 14,100 years ago.
- General considerations of $\delta^{18}\text{O}$ in water vapor and precipitation are reviewed by W. Dansgaard *et al.* (2), J. Gat [in *Handbook of Environmental Isotope Geochemistry*, P. Fritz and J. Ch. Fontes, Eds. (Elsevier, Amsterdam, 1980), vol. 1, pp. 21–48], and J. Jouzel (*ibid.*, vol. 2, pp. 61–112).
- S. J. Johnsen *et al.* (1) and R. Alley *et al.* (6) argue that the modern $\delta^{18}\text{O}$ -temperature relation over Greenland may be used to interpret the past ice core record. R. G. Fairbanks [*Nature* **342**, 637 (1989); (25)] cautions that moisture source variability and air mass mixing may have dominated certain abrupt changes in the ice cores.
- S. Joussame and J. Jouzel [*J. Geophys. Res.* **98**, 2807 (1993)] found that the slope of the $\delta^{18}\text{O}$ -temperature relation in an ice age GCM experiment differed from the modern observed value over Greenland by about 30%.
- A full description of the GISS II model and the basic parameterizations is provided by J. Hansen *et al.* [*Mon. Weather Rev.* **111**, 609 (1983)].
- CLIMAP Project Members, *Science* **191**, 1131 (1976); *Geol. Soc. Am. Map and Chart Ser. MC-36* (1981). Revisions to the boundary conditions used in this report may be necessary for more accurate simulations. In particular, recent evidence suggests that sea ice limits [N. Koç *et al.*, *Quat. Sci. Rev.* **12**, 115 (1993)] and tropical SSTs (T. Guilderson *et al.*, *Science*, in press) may need adjustment.
- A description of the isotope model and the results of the modern control experiment (8° by 10° resolution) are presented in J. Jouzel *et al.*, *J. Geophys. Res.* **92**, 14739 (1987). A complete description of the relevant parameterizations, as well as the results of various sensitivity tests, can be found in J. Jouzel *et al.*, *ibid.* **96**, 7495 (1991).
- S. Joussame *et al.*, *Ocean-Air Interactions* **1**, 43 (1986); R. D. Koster *et al.*, *Geophys. Res. Lett.* **13**, 121 (1986); R. D. Koster *et al.*, *Mass. Inst. Technol. Technol. Rep.* **317** (1988).
- S. Johnsen *et al.*, *Tellus* **41**, 452 (1989).
- L. M. Druyvan and D. Rind, *Natl. Aeronaut. Space Admin. Technol. Memo.* **100722** (1989).
- W. L. Gates, P. R. Rowntree, Q.-C. Zeng, in *Climate Change: The IPCC Scientific Assessment*, J. T. Houghton, G. J. Jenkins, J. J. Ephraums, Eds. (Cambridge Univ. Press, Cambridge, 1990), pp. 93–130. The fact that similar overestimation of Greenland precipitation appears in different models suggests that the error is not strictly the result of numerical diffusion, which is always a concern in the polar regions.
- It is apparent that mid-latitude $\delta^{18}\text{O}$ -temperature relations for the model match observations remarkably well, both over continents and over the oceans. R. Koster *et al.* [*Geophys. Res. Lett.* **20**, 2215 (1993)] have recently demonstrated that much of the scatter in the $\delta^{18}\text{O}$ -temperature relation in the coarse resolution model can be explained by the degree of continental recycling of moisture.
- N. Reeh, in *Geological History of the Polar Oceans: Arctic versus Antarctic*, U. Bleil and J. Thiede, Eds. (Kluwer, Dordrecht, Netherlands, 1990), pp. 255–272; see also (6).
- S. J. Johnsen *et al.* (1) give a table with the average amplitude of $\delta^{18}\text{O}$ variations in the different ice cores. The issue of what sets the Camp Century core apart—including arguments for and against ice elevation changes as a significant influence—has been discussed by W. Dansgaard *et al.* [*Geophys. Monogr. Ser.* **29** (American Geophysical Union, Washington, DC, 1984)] and N. Reeh *et al.* [*Paleogeogr. Paleoclimatol. Paleoecol.* **90**, 373 (1991)]. R. G. Fairbanks (25) also discussed this subject in light of possible changes in evaporative moisture sources.
- J. Kutzbach, in *North America and Adjacent Oceans During the Last Deglaciation*, W. F. Ruddiman and H. E. Wright Jr., Eds. (Geological Society of America, Boulder, CO, 1990).
- K. Taylor *et al.*, *Nature* **361**, 463 (1993).
- R. D. Koster *et al.*, *Clim. Dyn.* **7**, 195 (1992); also see (15).
- R. G. Fairbanks, *Paleoceanography* **5**, 937 (1990).
- This work was made possible by a National Research Council postdoctoral fellowship (C.D.C.). We appreciate the assistance and expertise provided by numerous collaborators at NASA/GISS, especially M. Chandler, R. Ruedy, B. Suzzo, and R. Webb. Discussions with W. Broecker, J. Cole, and D. Peteet were helpful, as were the comments made by two anonymous reviewers of a previous version of the manuscript.

27 July 1993; accepted 10 November 1993

Large First Hyperpolarizabilities in Push-Pull Polyenes by Tuning of the Bond Length Alternation and Aromaticity

Seth R. Marder,* Lap-Tak Cheng, Bruce G. Tiemann, Andrienne C. Friedli, Mireille Blanchard-Desce, Joseph W. Perry, Jørgen Skindhøj

Conjugated organic compounds with 3-phenyl-5-isoxazolone or *N,N'*-diethylthiobarbituric acid acceptors have large first molecular hyperpolarizabilities (β) in comparison with compounds with 4-nitrophenyl acceptors. For example, the julolidinyl-(CH=CH)₃-CH=N,*N'*-diethylthiobarbituric acid, which has 12 atoms between the donor and acceptor, has a $\beta(0)$ of 911×10^{-30} electrostatic units, whereas (CH₃)₂NC₆H₄-(CH=CH)₄-C₆H₄NO₂, with 16 atoms between its donor and acceptor, has a $\beta(0)$ of 133×10^{-30} electrostatic units. The design strategies demonstrated here have resulted in chromophores that when incorporated into poled-polymer electrooptic modulators exhibited significant enhancements in electrooptic coefficients relative to polymers containing the commonly used dye Disperse Red-1. Poled polymer devices based on these or related chromophores may ultimately lead to high-speed electrooptic switching elements with low drive-power requirements, suitable for telecommunications applications.

There is currently a concerted effort in industry, academia, and government laboratories to develop high-performance electrooptic switching elements for telecommunications, optical information processing, and sensors, based on poled polymers containing organic second-order nonlinear optical (NLO) chromophores. Substantial progress has been made in demonstrating that stable, optical quality devices can be fabricated. However, dramatic improvements in the electrooptic coefficients are required if these devices

are to have wide-ranging application in photonic systems. This realization has created a pressing need for organic chromophores with an order-of-magnitude increase in the molecular first hyperpolarizability, β , over those of commonly used chromophores, such as the well-known Disperse Red-1. We synthesized chromophores with greatly enhanced β by a basic design strategy that was proposed earlier (1) and is outlined below.

With a two-state model (2–4), it was shown that there is an optimal combina-